LRR-BASED HYPERSPECTRAL IMAGE RESTORATION BY EXPLOITING THE UNION STRUCTURE OF SPECTRAL SPACE AND WITH ROBUST DICTIONARY ESTIMATION

Mengdi Wang[1]*, Jing Yu*[2]*, Weidong Sun*[1]

1. State Key Lab. of Intelligent Technology and Systems,
Tsinghua National Lab. for Information Science and Technology,
Dept. of Electronic Engineering, Tsinghua Univ., Beijing 100084, China
2. Faculty of Information Technology, Beijing Univ. of Technology, Beijing 100124, China

ABSTRACT

Hyperspectral images (HSIs) are often corrupted by noises during acquisition, so the restoration of noisy HSIs is an essential procedure for the following applications. Low-rank representation (LRR) gives us a very powerful tool to detect the subspace singularity of hyperspectral data, but how to find a suitable subspace which better ensure the low-rank property and how to build a more robust dictionary to fit with the LRR framework are still open problems. Here in this paper, a novel LRR-based HSI restoration method by exploiting the union structure of spectral space and with robust dictionary estimation is proposed. In this method, the spectral space is represented by a union structure of several low-rank subspaces according to different land-covers and the dictionary is estimated using the robust principle component analysis (RPCA) to guarantee the LRR framework is more robust with the corruption noises. Experiments conducted on both simulated and real data show that our method achieves great improvement over the state-of-art methods qualitatively and quantitatively.

Index Terms— Hyperspectral image, restoration, low rank representation, robust principle component analysis.

1. INTRODUCTION

Hyperspectral images (HSIs) can provide both spatial and spectral information of the land-covers in a scene and therefore are widely used in various fields, including agriculture, environmental monitoring, food safety and mineralogy. However, the noises in the acquisition procedure can degrade the quality of HSIs and are harmful to the subsequent tasks, such as classification, spectral unmixing and target detection.

There are lots of outstanding works conducted on HSI restoration. Traditional methods for the restoration of natural images can be applied to HSIs band-by-band theoretically. However they ignore the spectral correlation information, which is an important characteristic of HSIs. Recently, much more methods are proposed to employ the spatial and spectral information simultaneously. Othman *et al.* [1] introduced a wavelet shrinkage method in the hybrid spatial-spectral derivative domain. Zhang *et al.* [2] proposed a cubic total variation (CTV) regularization to HSI restoration and [3] improved it to be spectral-spatial adaptive. Renard *et al.* [4] introduced a low rank-(K_1, K_2, K_3) tensor approximation method for dimensionality reduction and joint denoising. Guo *et al.* [5] proposed to use rank-1 tensor decomposition (R1TD) for HSI restoration, which is also called generalized-PCA in high order dimension. Most recently, Xie *et al.* [6] proposed a multispectral image restoration method with intrinsic tensor sparsity (ITS) regularization, which simultaneously considered the global spectral correlation and the nonlocal spatial similarity. RPCA-based method is introduced by Zhang *et al.* [7], under the constraint that the spectral space of HSIs should be low-rank. Our recent work [8] improved this method by introducing non-local spatial similarity through group combination of similar patches.

However, the RPCA-based methods [7–9] conduct no constraints on the inner structure of the low-rank spectral space. Actually, the spectral space of HSIs can be represented as a union of multiple low-rank subspaces according to different land-covers instead of a single low-rank space. The framework of LRR [10] provided a powerful tool to recover the union structure from noise and outlier corruption. For reconstruction of the spectral space, here we propose an HSI restoration method based on LRR. LRR is firstly proposed by Liu *et al.* [10] for subspace segmentation and now is widely used in multiple domains [11–15]. As stated in [10], with a proper dictionary, LRR can reconstruct the union structure from outliers and noises robustly. However, the choice of dictionary is still an open problem. A robust dictionary procedure is also proposed in this paper. In the proposed method, different from traditional LRR methods who always use the corrupted data itself as the dictionary [10–15], we introduce a dictionary estimation procedure using RPCA to guarantee that LRR is more robust with the noises.

The rest of this paper is organized as follows. Section 2

This work was supported by the National Nature Science Foundation (61501008) of China and the Natural Science Foundation of Beijing (4172002).

introduces our proposed method detailed. Experimental results and discussion are shown in Section 3, and Section 4 draws the conclusion.

2. THE PROPOSED METHOD

2.1. Union structure of the spectral space

To explore the inner structure of the spectral space, we should consider the property of the subspaces. The spectral space can be divided into multiple subspaces according to different criterion, but for the restoration problem, division that can guarantee the subspaces are compact and separable from noises should be adopted. Here we propose to divide the space according to the land-covers to guarantee the subspace is low-rank and thus lie in a compact low-dimension manifold.

The pixels of HSIs can be divided into several classes according to the land-covers and the spectral vectors within each class share high similarity thus lying in a low-dimension manifold. Therefore the whole spectral space can be represented as the union of such low-rank subspaces $\bigcup_{i=1}^{K} \mathcal{S}_i$, where $\mathcal{S}_i$ denotes the subspace of class $i\,(i = 1, \ldots, K)$. RPCA-based methods only conduct low-rank constraint on the whole space, which actually means that the space spanned by such subspaces should be low-rank, while the spanned space can be represented by the sum $\sum_{i=1}^{K} \mathcal{S}_k$. Difference between the union and the sum of subspaces is shown in Fig. 1. As the sum space is much larger than the union, the recovery using RPCA-based methods may be inaccurate. Therefore a better framework who could consider the subspace singularity and the union structure should be adopted.

2.2. LRR-based restoration method

2.2.1. *LRR framework*

The noises in HSIs can be divided into two classes according to their distribution: sparse noise and dense noise, where sparse noise mainly contains the salt-and-pepper noise and the stripe noise, and dense noise is typically the Gaussian noise. Therefore the observed HSI $\mathbf{X} \in \mathbb{R}^{B \times P}$(which is reorganized from the HSI datacube $\mathcal{X} \in \mathbb{R}^{M \times N \times B}$ with $P = MN$), where B is the band number and P is the pixel number, can be modelled as,

$$\mathbf{X} = \mathbf{X}_0 + \mathbf{S} + \mathbf{N}, \tag{1}$$

where $\mathbf{X}_0$ is the latent clean HSI to be recovered, $\mathbf{S}$ is the sparse noise and $\mathbf{N}$ is the Gaussian noise. To recover the union structure within $\mathbf{X}_0$, we introduce the LRR framework. In LRR, the union structural data $\mathbf{X}_0$ is modelled as

$$\mathbf{X}_0 = \mathbf{D}\mathbf{Z}, \tag{2}$$

where $\mathbf{D}$ is a dictionary that can well represent the subspace structure of $\mathbf{X}_0$, and $\mathbf{Z}$ is low-rank. Combining the constraint

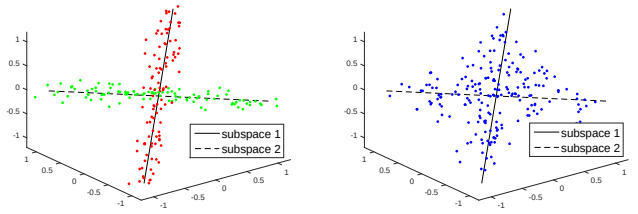

(a) Union ($\bigcup_{i=1}^{2} \mathcal{S}_i$) (b) Sum ($\sum_{i=1}^{2} \mathcal{S}_i$)

Fig. 1. Difference between the union and sum of subspaces

in Eq.(1), the inverse optimization function of Eq.(2) is

$$\min_{\mathbf{Z},\mathbf{S}} \ \mathrm{rank}\,(\mathbf{Z}) + \lambda\|\mathbf{S}\|_0 + \frac{\gamma}{2}\|\mathbf{X} - \mathbf{D}\mathbf{Z} - \mathbf{S}\|_{\mathrm{F}}^2, \tag{3}$$

where $\mathrm{rank}\,(\mathbf{Z})$ conducts constraint on the rank of coefficient matrix $\mathbf{Z}$, $\|\mathbf{S}\|_0$ is the regularization of the sparse noise using ℓ_0-norm, and $\|\mathbf{X} - \mathbf{D}\mathbf{Z} - \mathbf{S}\|_{\mathrm{F}}^2$ is the fidelity item, conducting constraint upon the energy level of Gaussian noise $\mathbf{N}$, λ and γ are balance parameters. As rank minimization and ℓ_0-norm are nonconvex, a common practice is to replace them with the nuclear norm and ℓ_1-norm, respectively,

$$\min_{\mathbf{Z},\mathbf{S}} \ \|\mathbf{Z}\|_* + \lambda\|\mathbf{S}\|_1 + \frac{\gamma}{2}\|\mathbf{X} - \mathbf{D}\mathbf{Z} - \mathbf{S}\|_{\mathrm{F}}^2, \tag{4}$$

Eq.(4) can be solved using the inexact augmented Lagrange multiplier (IALM) method [16]. Restored HSI can be obtained by $\hat{\mathbf{X}}_0 = \mathbf{D}\mathbf{Z}^*$, with $\mathbf{Z}^*$ being the optimal solution of Eq.(4).

2.2.2. *Estimation of the dictionary*

It is demonstrated in [10] that if the dictionary $\mathbf{D}$ is exactly sampled from the union structure, minimization of $\|\mathbf{Z}\|_*$ can guarantee the recovery of the column space of the latent clean data from noises. In traditional LRR methods [10–15], self-representation is always adopted, which means that the data $\mathbf{X}$ itself is used as the dictionary. However in HSI restoration problem, $\mathbf{X}$ is seriously corrupted. The subspace structure is severely corrupted which may lead to inaccuracy of the self-representation. A more robust choice of the dictionary is needed. [11] proposed a closed-form for the dictionary estimation, which used the latent clean data $\mathbf{X}_0$ as the dictionary and estimated it iteratively during the solution. However, experiments show that the improvement is quite limited. In this paper we propose to robustly estimate the dictionary using RPCA. RPCA conducts low-rank constraint on the whole space,

$$\min_{\mathbf{X}_0,\mathbf{S}} \ \|\mathbf{X}_0\|_* + \alpha\|\mathbf{S}\|_1 + \frac{\beta}{2}\|\mathbf{X} - \mathbf{X}_0 - \mathbf{S}\|_{\mathrm{F}}^2, \tag{5}$$

where α and β are balance parameters. RPCA can reduce the noises outside the sum space $\sum_{i=1}^{K} \mathcal{S}_k$. The estimated result

is much closer to the real spectral structure than the original noisy data $\mathbf{X}$, thus is much more robust with the corruption noises. The robustness will be demonstrated by the experiments in Section 3 by setting the dictionary as $\mathbf{D} = \mathbf{X}$ and $\mathbf{D} = \hat{\mathbf{X}}_{\text{RPCA}}$, where $\hat{\mathbf{X}}_{\text{RPCA}}$ is the result obtained using Eq.(5).

3. EXPERIMENTAL RESULTS AND DISCUSSION

In the experiments, clean data added with simulated noises and real-world noisy data are both used. The subjective and objective assessment results are shown for both experiments. To demonstrate the effectiveness of the proposed method, we compare our method with RPCA [7], G-RPCA [8], ITS [6]. As ITS only considers the Gaussian noise and did not take the sparse noises into consideration, for fairness of comparison when dealing with complex noises, we compare with ITS extensively by firstly minimizing the sparse noises roughly using RPCA and then using ITS to reduce the dense noises. This method is called as RPCA-ITS. Two LRR-based method are evaluated, sLRR and rLRR, while sLRR uses the self-representation dictionary $\mathbf{D} = \mathbf{X}$ and rLRR uses the robust estimated dictionary $\mathbf{D} = \hat{\mathbf{X}}_{\text{RPCA}}$. The comparison between sLRR and rLRR can show the robustness obtained by our proposed dictionary estimation procedure. Optimal parameters are used for all the methods.

3.1. Experiments on the simulated data

In the simulated experiments, the HSI of Pavia University acquired by the reflective optics system imaging spectrometer (ROSIS) is used (called as *Pavia University* for brief in the following). This data contains 103 bands, with a spatial size of 610×340. We simulate three kinds of typical noises in the experiments: the Gaussian noise, the salt-and-pepper noise and the stripe noise. The stripe noise often appears in push-broom systems. In the simulated data, the Gaussian noise with $\sigma = 5\%$ are added to all the bands; in addition: 1) 8 bands are corrupted by the salt-and-pepper noise with a percentage of 20%, 2) 8 bands are corrupted by the stripe noise with random 10-line stripes, 3) 2 bands are corrupted both by the salt-and-pepper noise and stripe noise. Fig.2 (a) and (b) show the original and the corresponding noisy image of band 53, which is corrupted by all the three types of noises.

The restored results are shown in Fig.2. The close-up of the area in the red rectangle is shown in the bottom-right corner. From Fig. 2 we can see that rLRR performs best among all the methods. RPCA and G-RPCA both remove the stripe noise, but fails on the elimination of the salt-and-pepper noise and Gaussian noise. ITS performs worst on this band, as it ignores the sparse noises in its model. RPCA-ITS performs much better as the sparse noises are firstly removed by RPCA, however ITS can still not remove the remaining noises thoroughly and at the same time it oversmoothes some area, such as the top-right part in the close-up area. The strip noise is not eliminated thoroughly by sLRR. Our method can remove all the noises and restore the spatial details well.

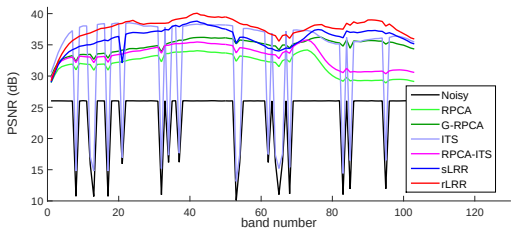

(a) PSNR

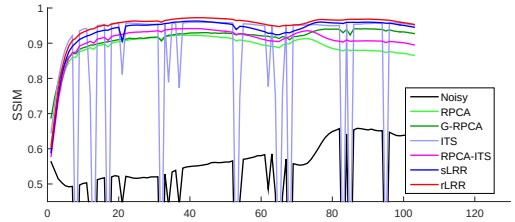

(b) SSIM

Fig. 3. Quantitative evaluation of the six methods.

To further evaluate the restoration performance of all the methods, peak signal-to-noise ratio (PSNR) and structural similarity (SSIM) [17] are adopted. Both indices are calculated band-by-band and both indicate better performance with higher values. Fig. 3 shows the results. ITS performs quite well on the bands only with Gaussian noise, with some bands even better than rLRR. But, it fails on the bands with sparse noises. RPCA-ITS performs much better and even shows improvement upon RPCA. On average sLRR and rLRR performs the best, showing the benefits from the LRR framework. rLRR is even better, and additionally sLRR fails in several bands with sparse noises, which could illustrate the robustness obtained by the proposed dictionary estimation procedure.

Table 1 shows the classification results of the restored data by all the six methods. The support vector machine (SVM) with radius basis function (RBF) is used as the classification method. The optimal parameters are chosen using fivefold cross-validation. 1% of samples are used as the training data and the remaining as the testing data. The classification experiments are repeated for 10 times and the average results are shown, including average accuracy (AA), overall accuracy (OA) and Kappa coefficient (κ). We can observe that rLRR achieves the highest AA, OA and also κ.

Table 1. Classification results (%) using SVM

	RPCA	G-RPCA	ITS	RPCA-ITS	sLRR	rLRR
AA	72.40	87.38	78.20	93.86	93.40	**94.74**
OA	61.75	76.45	68.35	86.14	84.60	**87.26**
κ	0.63	0.83	0.71	0.91	0.91	**0.93**

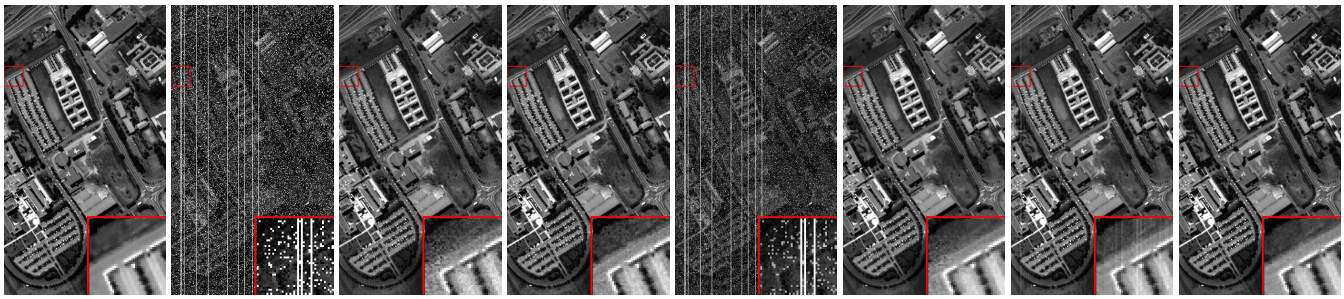

(a) original band (b) noisy band (c) RPCA [7] (d) G-PRCA [8] (e) ITS [6] (f) RPCA-ITS (g) sLRR (h) rLRR

Fig. 2. Experimental Results of band 53 in the simulated Pavia University data.

(a) original band (b) RPCA [7] (c) G-RPCA [8] (d) ITS [6] (e) RPCA-ITS (f) sLRR (g) rLRR

Fig. 4. Experimental results of band 104 in Urban

3.2. Experiments on the real data

A hyperspectral digital collection experiment (HYDICE) data, Urban of Copperas Cove, Texas (called as *Urban* for brief in the following) is used in our experiments as the real noisy data. The spatial and spectral size of Urban are 307×307 and 210. 22 bands are removed from the original data because these bands cannot provide any useful information due to the pollution by atmosphere and water absorption. In Urban, several bands are corrupted by heavy noises, such as band 104 shown in Fig. 4(a).

Figs. 4(b)-(g) show the restored results by the six methods, with the sub-image in the bottom-right corner showing the close-up of the area in the red rectangle. It can be observed that all the methods besides rLRR fails to remove the stripe noise thoroughly. In addition, ITS and RPCA-ITS have the effect of oversmoothness. Our proposed method rLRR performs much better on the elimination of the noises and on the restoration of the spatial structures at the same time.

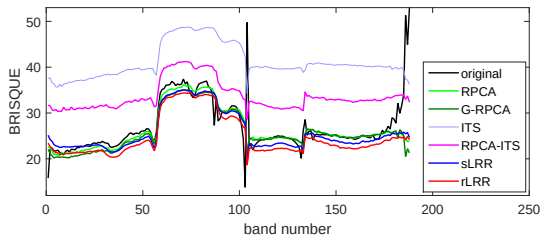

Fig. 5. BRISQUE results in Urban.

To objectively evaluate the restored result of the proposed method, objective assessment indices should be used. However, both PSNR and SSIM need a reference image, therefore they are not applicable for the real noisy data. In this part, blind/referenceless image spatial quality evaluator (BRISQUE) [18] is employed, as it is a widely-used no-reference image evaluation index. For BRISQUE, smaller number indicates better performance. The results are shown in Fig.5. It can be observed that our method rLRR performs the best, while ITS and RPCA-ITS performs even worse than the original data, which can also be indicated from Fig.4 (d) and (e) as they oversmooth the band.

4. CONCLUSION

In this paper, we have proposed a LRR-based HSI restoration method through exploiting the union structure of the spectral space, and furthermore a robust dictionary estimation procedure. In this method, considering inner structure of the spectral space, the framework of LRR is employed to reconstruct the corrupted union structure of multiple subspaces and a robust dictionary estimation procedure using RPCA is adopted. Comparison between LRR-based methods (including sLRR and rLRR) and the other methods shows the effectiveness of the appropriate employment of the union spectral structure through LRR. Improvement of rLRR upon sLRR illustrates the robustness achieved by the dictionary estimation procedure. Experimental results both on simulated and real-world noisy HSI data demonstrate that, our proposed method outperforms the state-of-art methods.

5. REFERENCES

[1] H. Othman and S.E. Qian, "Noise reduction of hyperspectral imagery using hybrid spatial-spectral derivative-domain wavelet shrinkage," *IEEE Trans. Geosci. Remote Sens.*, vol. 44, no. 2, pp. 397–408, Feb 2006.

[2] H. Zhang, "Hyperspectral image denoising with cubic total variation Model," *ISPRS Ann. Photogramm., Remote Sens. Spatial Inf. Sci.*, pp. 95–98, July 2012.

[3] Q. Yuan, L. Zhang, and H. Shen, "Hyperspectral image denoising employing a spectral-spatial adaptive total variation model," *IEEE Trans. Geosci. Remote Sens.*, vol. 50, no. 10, pp. 3660–3677, Oct 2012.

[4] N. Renard, S. Bourennane, and J. Blanc-Talon, "Denoising and dimensionality reduction using multilinear tools for hyperspectral images," *IEEE Geosci. Remote Sens. Lett.*, vol. 5, no. 2, pp. 138–142, April 2008.

[5] X. Guo, X. Huang, L. Zhang, and L. Zhang, "Hyperspectral image noise reduction based on rank-1 tensor decomposition," *ISPRS J. Photogramm. and Remote Sens.*, vol. 83, no. 0, pp. 50–63, 2013.

[6] Qi Xie, Qian Zhao, Deyu Meng, Zongben Xu, Shuhang Gu, Wangmeng Zuo, and Lei Zhang, "Multispectral images denoising by intrinsic tensor sparsity regularization," in *CVPR*, 2016.

[7] H. Zhang, W. He, L. Zhang, H. Shen, and Q.Yuan, "Hyperspectral image restoration using low-rank matrix recovery," *IEEE Trans. Geosci. Remote Sens.*, vol. 52, no. 8, pp. 4729–4743, Aug 2014.

[8] M. Wang, J. Yu, J. H. Xue, and W. Sun, "Denoising of hyperspectral images using group low-rank representation," *IEEE J. Sel. Topics Appl. Earth Observ. in Remote Sens.*, vol. 9, no. 9, pp. 4420–4427, Sept 2016.

[9] M. Wang, J. Yu, and W. Sun, "Group-based hyperspectral image denoising using low rank representation," in *Proc. ICIP*. IEEE, 2015, pp. 1623–1627.

[10] G. Liu, Z. Lin, S. Yan, J. Sun, Y. Yu, and Y. Ma, "Robust recovery of subspace structures by low-rank representation," *IEEE Trans. Pattern Anal. Mach. Intell.*, vol. 35, no. 1, pp. 171–184, Jan 2013.

[11] P. Favaro, R. Vidal, and A. Ravichandran, "A closed form solution to robust subspace estimation and clustering," in *Proc. IEEE Conf. Comput. Vis. Pattern Recognit.*, June 2011, pp. 1801–1807.

[12] C. Lang, G. Liu, J. Yu, and S. Yan, "Saliency detection by multitask sparsity pursuit," *IEEE Trans. Image Process.*, vol. 21, no. 3, pp. 1327–1338, March 2012.

[13] B. Cheng, G. Liu, J. Wang, Z. Huang, and S. Yan, "Multi-task low-rank affinity pursuit for image segmentation," in *Proc. IEEE Int. Conf. Comput. Vis.*, Nov 2011, pp. 2439–2446.

[14] Alex Sumarsono and Qian Du, "Low-rank subspace representation for estimating the number of signal subspaces in hyperspectral imagery," *IEEE Trans. Geosci. Remote Sens.*, vol. 53, no. 11, pp. 6286–6292, 2015.

[15] X. Lu, Y. Wang, and Y. Yuan, "Graph-regularized low-rank representation for destriping of hyperspectral images," *IEEE Trans. Geosci. Remote Sens.*, vol. 51, no. 7, pp. 4009–4018, Jul. 2013.

[16] Z. Lin, M. Chen, and Y. Ma, "The augmented lagrange multiplier method for exact recovery of corrupted low-rank matrices," in *arXiv preprint arXiv:1009.5055*, 2010.

[17] Z. Wang, A.C. Bovik, H.R. Sheikh, and E.P. Simoncelli, "Image quality assessment: from error visibility to structural similarity," *IEEE Trans. Image Process.*, vol. 13, no. 4, pp. 600–612, Apr 2004.

[18] A. Mittal, A. K. Moorthy, and A. C. Bovik, "No-reference image quality assessment in the spatial domain," *IEEE Trans. on Image Process.*, vol. 21, no. 12, pp. 4695–4708, Dec 2012.